

## Low-Frequency Raman Study of Drawn Polyethylene

R. G. Snyder\*

Department of Chemistry, University of California, Berkeley, California 94720, and  
Western Regional Research Center, Science and Education Administration,  
U.S. Department of Agriculture, Berkeley, California 94710

J. R. Scherer

Western Regional Research Center, Science and Education Administration,  
U.S. Department of Agriculture, Berkeley, California 94710

A. Peterlin

Center for Materials Science, National Bureau of Standards, Washington, D.C. 20234.  
Received May 13, 1980

**ABSTRACT:** The low-frequency Raman spectrum of unannealed, drawn (20 $\times$ , 60 °C) polyethylene displays a LAM-1 band whose shape and breadth are extraordinary relative to LAM-1 for other forms of crystalline polyethylene. From the shape of this band a distribution of lengths of straight-chain segments was derived. A value of 90 Å was obtained for the most probable length of an extended segment. This value is about one-half that of the long period determined for similar drawn samples using small-angle X-ray scattering. Part of the difference between the Raman and SAXS values may be accounted for in terms of the breadth and asymmetry of the distribution of straight-chain segment lengths. The presence of a large concentration of straight-chain segments having lengths less than 100 Å and the unusual breadth of the distribution relative to the most probable length indicate a fundamental difference between the morphology of the unannealed drawn sample and that of solution- or melt-crystallized samples. The distribution of lengths displays a tail that is probably associated with tie chains. Annealing the sample moves the distribution curve to longer lengths and broadens it although its general shape and the high degree of alignment of chains parallel to the fiber axis are preserved.

## Introduction

The unique properties of polyethylene in the drawn state and the diversity of models proposed to explain them<sup>1</sup> make this material a particularly appropriate subject for study by new structural methods. In this paper we report on a low-frequency Raman investigation of the morphology of a highly drawn polyethylene fiber. One kind of morphological information that can be determined by this technique is an approximate distribution of the lengths of straight-chain segments, i.e., lengths of segments that are fully extended. This distribution can be derived from the shape of the LAM-1 (longitudinal acoustic mode,  $k = 1$  member) band as has been described earlier in a study on the extrudate of this same polymer.<sup>2</sup>

Much of what is known at the molecular level about long-range order in drawn samples has resulted from diffraction studies, particularly those involving small-angle X-ray scattering (SAXS). The Raman method differs from SAXS in its sensitivity to long-range conformational order associated with single chains and its insensitivity to long-range structural periodicity. For SAXS the reverse situation occurs. Hence the two techniques yield complementary data. For well-ordered systems such as solution-crystallized polyethylene, the observed value of the periodicity of the crystal-amorphous alternation determined by SAXS is normally close to the most probable length of the straight-chain segments determined by the Raman method after account has been taken for the possibility of chain tilt.<sup>3,4</sup> For the drawn sample studied here, however, the SAXS periodicity is nearly twice the most probable straight-chain length determined from an analysis of the LAM-1 band. Possible reasons for the large difference between these values will be discussed.

In this paper we will use  $L$  to denote the length of a straight-chain segment determined by Raman scattering and  $\ell$  to denote the long period determined by SAXS.

## Experiment and Theory

Raman spectra were measured by using a computer-controlled double monochromator (Spex 1401) with a cooled photomultiplier

(RCA 31034A).<sup>24</sup> The control system, photon-counting system, and automated polarization analyzer have been previously described.<sup>5</sup> The high-intensity background associated with the exciting radiation (5145 Å) was largely removed by using an iodine-vapor cell in conjunction with a tuned etalon inside the cavity of the laser. Elimination of iodine lines from the spectrum was accomplished by ratioing, at successive frequency intervals, the intensity of radiation scattered from the sample and the intensity of radiation from a white-light source.<sup>6</sup> All spectra were measured with 1-cm<sup>-1</sup> slits.

The sample was prepared by drawing polyethylene at 60 °C to an extension ratio of 20 at a rate of 5 mm/min. The resulting fiber was about 0.2 mm by 1.0 mm in cross section.

A right-angle scattering geometry was employed. The sample, whose ends were semirigidly fixed, was positioned in front of the slit so that its draw axis  $c$  was perpendicular to the plane defined by the monochromator axis and the vertical path of the exciting radiation. Two kinds of spectra,  $cc$  and  $cd$ , were measured. For both, the excitation was polarized parallel to the  $c$  axis while the scattered light was either parallel ( $cc$  spectrum) or perpendicular ( $cd$  spectrum) to  $c$ . Since the polyethylene chains are highly oriented parallel to the fiber axis, the LAM-1 band could be isolated from its background by subtracting a scaled  $cd$  spectrum, which does not show LAM-1, from the  $cc$  spectrum. This procedure is described in more detail elsewhere.<sup>2</sup> It was unnecessary to deconvolute the observed LAM bands for slit effects since band half-width exceeded the slit width by at least a factor of 10.

The distribution of lengths of straight-chain segments is related<sup>2</sup> to the shape of the LAM-1 band according to

$$f(L) = C\nu^2 B_\nu I_\nu^{\text{obsd}} \quad (1)$$

where  $f(L)$  is the distribution,  $C$  is a constant,  $I_\nu^{\text{obsd}}$  is the observed Raman intensity of the LAM-1 band at frequency  $\nu$  (in wave-numbers), and  $B_\nu$  is a Boltzmann factor defined

$$B_\nu = 1 - \exp(-h\nu/kT) \quad (2)$$

where  $T$  is the temperature of the sample. The frequency of LAM-1 of an extended chain of length  $L$  is given approximately by

$$\nu = 3093/L \quad (3)$$

where  $\nu$  is in cm<sup>-1</sup> and  $L$  is in Å.<sup>2</sup>

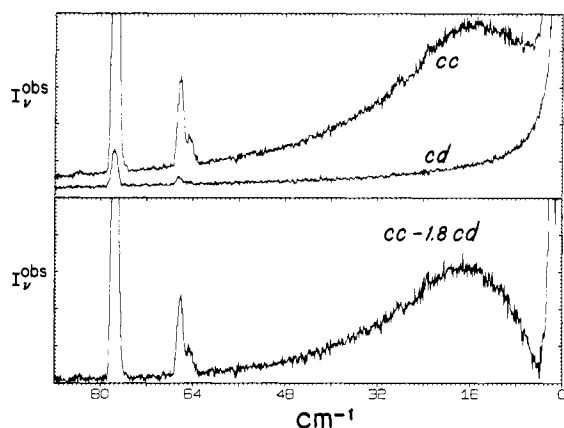


**Figure 1.** Observed low-frequency Raman spectra of a sample of unannealed drawn polyethylene at 26 °C (sample drawn 20X at 60 °C). At the top are the cc and cd spectra as measured; at the bottom is the cc spectrum corrected for background. (The bands near 78 and 66  $\text{cm}^{-1}$  are plasma lines.)

### Observed LAM-1 Spectra

**Unannealed Sample.** Polarized Raman spectra of an unannealed sample at room temperature in the region below 88  $\text{cm}^{-1}$  are shown at the top of Figure 1. The sharp bands near 78 and 66  $\text{cm}^{-1}$  result from laser plasma lines. The intense LAM-1 band near 16  $\text{cm}^{-1}$  appears in the cc spectrum but not in the cd spectrum due to the high degree of parallel alignment of the extended chains relative to the  $c$  axis.

Subtraction of a scaled cd spectrum from the observed cc spectrum gives the background-corrected spectrum at the bottom of Figure 1. We have used the highest value for the scaling factor that is possible without leading to negative intensity in the region near 4  $\text{cm}^{-1}$ . Although slightly smaller values for this factor may be admissible, their use would affect (increase) intensities significantly only in the region below 8  $\text{cm}^{-1}$ .

Compared with LAM-1 bands observed for other types of polyethylene, the LAM-1 band for the drawn sample is remarkably broad. Its half-width of 24  $\text{cm}^{-1}$  may be compared with a value near 7  $\text{cm}^{-1}$  for an extruded sample,<sup>2</sup> 5  $\text{cm}^{-1}$  for an unannealed solution-crystallized sample, and the maximum value of about 15  $\text{cm}^{-1}$  that is attained by annealing a solution-crystallized sample.<sup>7</sup>

A second unusual feature of this band is its asymmetry, the result of a long tail that extends to frequencies higher than 60  $\text{cm}^{-1}$ . The presence of this tail cannot be attributed to a high degree of conformational disorder for the following reasons. The dominant feature in the low-frequency region of the Raman spectra of conformationally disordered chains such as found for the long  $n$ -alkanes in the liquid state and for molten polyethylene is an intense broad band between 250 and 200  $\text{cm}^{-1}$ .<sup>8</sup> The spectrum of the drawn sample, both unannealed and annealed, does not display this band. In addition, bands in other regions of the Raman spectrum that are characteristic of conformational disorder are not observed for the drawn sample. Thus we conclude that the sample is highly ordered and crystalline, a conclusion that is in accord with results derived with other techniques.<sup>1</sup>

A background-corrected cc spectrum of the unannealed drawn sample is shown at the top of Figure 2. The same spectrum, after being converted through eq 1 to a distribution of straight-chain lengths, is shown at the bottom of this figure. Two additional stages of conversion, intermediate between these, are included to emphasize the fact that temperature and frequency corrections by themselves are responsible for most of the differences between

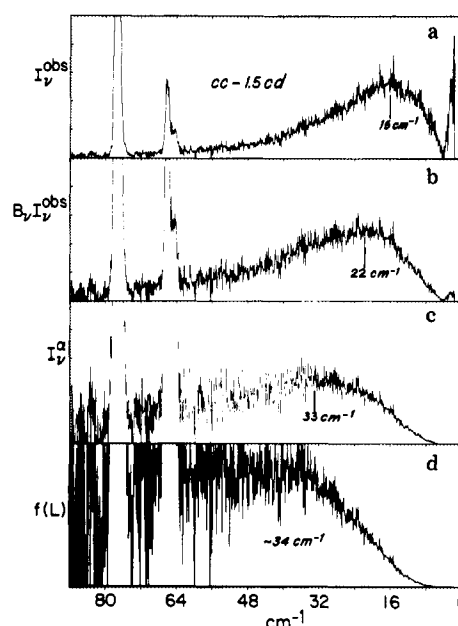


**Figure 2.** Raman spectrum of unannealed drawn polyethylene successively corrected. Starting from top: (a) background corrected; (b) Boltzmann-factor corrected; (c) expressed in terms of scattering activity; (d) expressed in terms of a distribution of lengths of straight-chain segments.

the observed spectrum and the spectrum expressed as a distribution of lengths. This is apparent when the relation between the observed intensity  $I_{\nu}^{\text{obsd}}$  and the Raman scattering activity  $I_{\nu}^{\alpha}$  is considered:

$$I_{\nu}^{\text{obsd}} = A \nu^{-1} B_{\nu}^{-1} I_{\nu}^{\alpha} \quad (4)$$

The scattering activity  $I_{\nu}^{\alpha}$ , integrated over the LAM-1 band, is directly related to elements of the derived polarizability tensor of the straight-chain segments and is essentially independent of temperature and frequency. It is therefore appropriate to express the Raman spectrum in terms of  $I_{\nu}^{\alpha}$ .<sup>9</sup> In Figure 2b the observed spectrum corrected for temperature is shown, and, in Figure 2c, the spectrum corrected for both temperature and frequency, i.e., expressed in terms of  $I_{\nu}^{\alpha}$ . We note that

$$f(L) = A \nu I_{\nu}^{\alpha} \quad (5)$$

which, when compared with eq 1, shows that the functions  $f(L)$  and  $I_{\nu}^{\alpha}$  are more closely related than are  $f(L)$  and  $I_{\nu}^{\text{obsd}}$ . We note also that in the sequence shown in Figure 2 the maximum moves to significantly higher frequencies (16, 22, 33, and  $>34$   $\text{cm}^{-1}$ ) at each step.

The distribution of straight-chain lengths as a function of  $L$  is shown in Figure 3. The data used to determine  $f(L)$  are those shown in Figure 2 corrected for the contribution of LAM-3 intensity to LAM-1. This contribution was estimated according to the procedure outlined in ref 2 and was significant at frequencies above 30  $\text{cm}^{-1}$ , i.e., for  $L < 100$  Å. As a result of this correction, the maximum of  $f(L)$  moved from about 80 to about 90 Å.

The uncertainty in  $f(L)$  resulting from experimental error in the measured Raman intensity, indicated in Figure 3 by the dashed line, becomes increasingly large in going to shorter straight-chain lengths. This occurs because at higher frequencies the uncertainty in the measurement of  $I_{\nu}^{\text{obsd}}$  increases and is in turn amplified by the factor  $\nu^2 B_{\nu}$  in eq 1. Consequently the value of  $f(L)$  is essentially undetermined for  $L < 80$  Å.

**Annealed Sample.** The spectrum of the sample at room temperature was measured before it was annealed

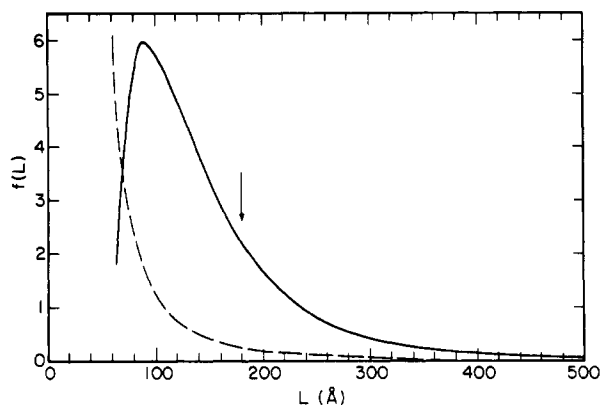


**Figure 3.** Distribution of lengths of straight-chain segments for unannealed drawn polyethylene derived from the spectrum shown in Figure 2. The long period determined by SAXS is indicated by the arrow. (The dashed line represents an estimate of the uncertainty in the distribution based on the  $S/N$  ratio in the spectrum. The units of  $f(L)$  are arbitrary.)

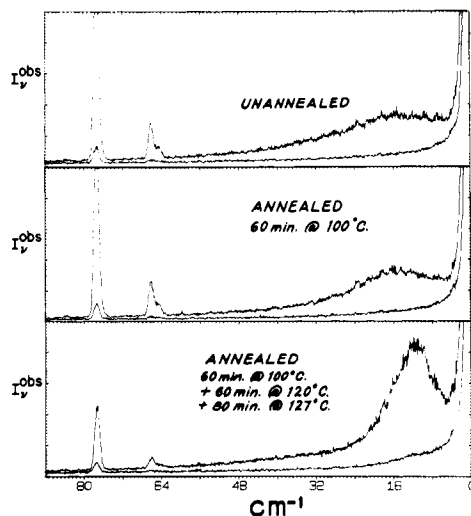


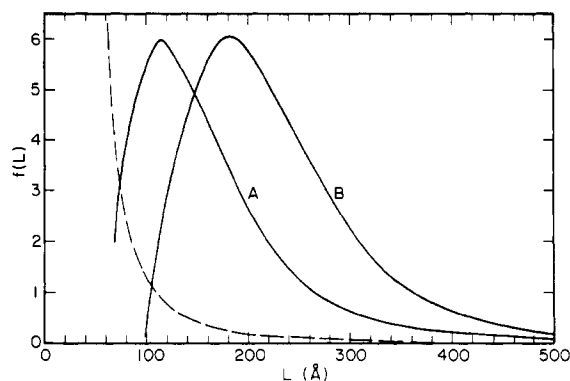
**Figure 4.** Observed low-frequency cc and cd Raman spectra of unannealed and annealed drawn polyethylene. Spectra are for the same sample successively annealed in situ.

and then again, in situ, each time after it was annealed at a higher temperature. During annealing the sample contracted slightly ( $\sim 5\%$ ). The resulting spectra are displayed in Figure 4, where it may be seen that, after annealing at the highest temperature, the sample scattered less of the exciting radiation, as evidenced by the loss of intensity in the laser plasma lines. Presumably this loss resulted from a reduction in the size or number of scattering voids in the sample. With regard to LAM-1, the effect of annealing was to shift its peak position to lower frequencies and to decrease its half-width. The distributions of straight-chain lengths shown in Figure 5 were derived from LAM-1 after it was corrected for LAM-3. These curves along with that for the unannealed sample (Figure 3) were arbitrarily scaled to give the same value at the maximum so that only the relative shapes of different distributions can be compared.

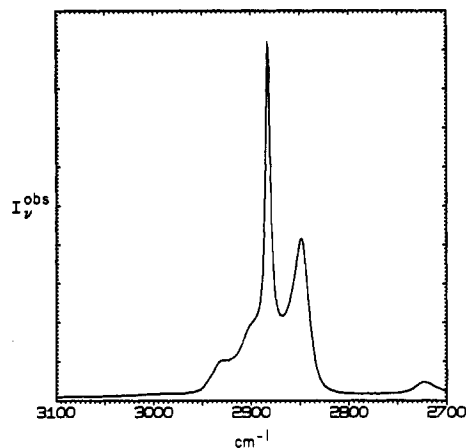
The peak positions and half-widths of LAM-1 and  $f(L)$  are listed in Table I for the unannealed and annealed samples.

### Chain Alignment

Chain alignment parallel to the draw axis can be measured by Raman or wide-angle X-ray (WAXS) methods. With a higher degree of alignment, the Raman method becomes more sensitive while the WAXS method becomes



**Figure 5.** Distribution of lengths of straight-chain segments for drawn annealed polyethylene derived from the spectra shown in Figure 4. Curve A is for the sample annealed at  $100^\circ\text{C}$  for 60 min; curve B is for the same sample further annealed at  $120^\circ\text{C}$  for 60 min and then at  $127^\circ\text{C}$  for 80 min. (The dashed line represents an estimate of the uncertainty in the distribution based on the  $S/N$  in the spectra. The units of  $f(L)$  are arbitrary.)



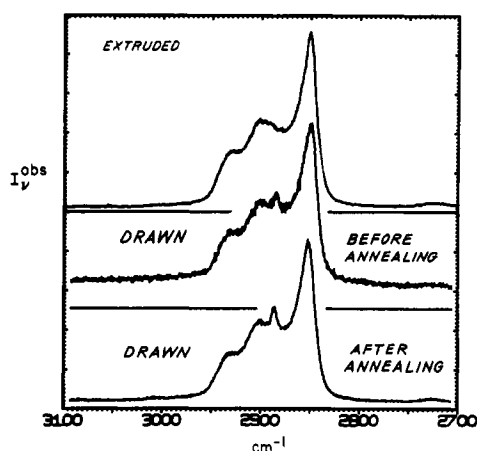
**Figure 6.** C-H stretching region of the Raman spectrum of a sample of randomly oriented solution-crystallized polycrystalline polyethylene.

Table I  
Observed LAM-1 Frequencies and Half-Widths (in  $\text{cm}^{-1}$ ) for Drawn Polyethylene and Peak Position and Half-Width of the Distribution of Lengths of Straight-Chain Segments (in Å)

	$\nu$	$\Delta\nu_{1/2}$	$L_{\text{max}}$	$\Delta L_{1/2}$
unannealed	16	24	90	90
annealed 60 min at $100^\circ\text{C}$	15.5	20	115	118
annealed 80 min at $127^\circ\text{C}$	11	11	182	155

less so. The low-frequency Raman spectra of the drawn sample, both unannealed and annealed, indicate a high degree of chain alignment. However, quantitative measurement in this region is difficult. In principle, the ratio of the intensity of LAM-1 in the cd spectrum to that in the cc spectrum can be used as a quantitative measure of chain alignment since, for the case of perfect alignment, LAM-1 will not appear in the cd spectrum at all. However, LAM-1 is very broad and its intensity is difficult to determine.

To measure chain alignment we used the 2885- and 2850- $\text{cm}^{-1}$  C-H stretching bands which are shown in Figure 6 for a sample of randomly oriented polycrystalline polyethylene. The ratio of the intensities of these two bands is a measure of alignment since the 2885- $\text{cm}^{-1}$  band is not allowed in the cc spectrum when all chains are parallel to  $c$ .<sup>10,11</sup> This may be seen in Figure 7 for a sample of ex-



**Figure 7.** C-H stretching region of the cc spectra of highly oriented polyethylene: extruded; unannealed drawn; annealed (127 °C) drawn.

truded polyethylene which is highly aligned. Also shown in this figure are the cc spectra of a drawn sample, both unannealed and annealed. We note that the relatively narrow 2885-cm<sup>-1</sup> band is superimposed on an unrelated intense and broad band.<sup>10</sup> Contributions from this broad background were excluded in determining the peak intensity of the 2885-cm<sup>-1</sup> band.

The relative intensities of the 2885- and 2850-cm<sup>-1</sup> bands indicate that the chains in the fiber are highly aligned, although somewhat less so than in the case of the extrudate. It appears that the process of annealing has little effect on the degree of alignment.

A quantitative estimate of alignment may be derived from the value of the peak-height intensity ratio  $I(2885)/I(2850)$  (which we designate as  $r$ ), provided we assume a one-parameter model that describes an alignment distribution. Two models were considered. The methods of computing the averages associated with these models are found in the Appendix.

In one model we assume that the system consists of two components, one having perfectly aligned chains and the other randomly aligned chains. The fraction of random chains necessary to give  $r$  a calculated value in the range of values (0.08–0.18) observed for the unannealed fiber is 3–7% and for the annealed fiber (129 °C), 4–9%.

A second model was considered in which all chains make the same angle  $\theta$  with the fiber axis. For the unannealed sample,  $\theta = 8$ –12° while for the annealed sample,  $\theta = 9$ –14°. For comparison, we estimate that  $\theta = 3$ –6° for the extrudate.

### Distribution of Lengths of Straight-Chain Segments

**Comparison with SAXS Measurements on the Unannealed Sample.** In the case of the unannealed sample, the distribution of lengths of straight-chain segments has its maximum  $L_{\max}$  in the region 80–100 Å. This length is approximately one-half the value of the long-spacing  $\ell$ , which is reported from SAXS measurements to be 180 Å.<sup>12</sup> This difference between the Raman and SAXS measurements is at variance with an earlier study on similar drawn samples which indicated that the length derived from LAM-1 was significantly greater than that from SAXS.<sup>13</sup> In this earlier work, however, the most probable length was computed from eq 3 by using the frequency at which  $I_{\nu}^{\text{obsd}}$  is a maximum. The value of  $L_{\max}$  derived in this manner will be significantly larger than that obtained from the distribution curve calculated with eq 1, in which case  $I_{\nu}^{\text{obsd}}$  is weighted by  $\nu^2 B_{\nu}$ .

The value of the most probable length of a straight-chain segment derived from the Raman measurement is essentially model independent. As we have seen earlier, if the observed Raman spectrum is corrected solely for frequency and temperature, i.e., not converted to a length distribution, the peak of the LAM-1 band corresponds to a chain length of about 95 Å (Figure 2). Conversion to  $f(L)$  reduces this value by only 5–15 Å. Thus, frequency and temperature corrections by themselves lead to a most probable length that is much less than the long period found by SAXS.

The situation for the drawn sample may be contrasted with that for solution- and melt-crystallized polyethylene. In these latter cases, approximate values of  $L_{\max}$  derived from eq 3 by using the peak frequency of LAM-1 and a value of the constant  $a$  in that equation determined from crystalline *n*-alkane LAM-1 frequencies are generally in good agreement with measured values of  $\ell$ .<sup>13,14</sup>

We will now consider some factors which, when taken into account, tend to reconcile  $L_{\max}$  and  $\ell$ .

We note that  $L_{\max}$  is the most likely value of the straight-chain segment length and not the average value  $L_{\text{av}}$  and that the average value is more closely related to the long period. Because  $f(L)$  is asymmetric,  $L_{\text{av}}$  is considerably larger than  $L_{\max}$  (Figure 3). We find  $L_{\text{av}}$  to be 125 Å. This value is probably on the low side because contributions from lengths larger than 300 Å were ignored and because, if our measurements are in error, this error will most likely have the effect of reducing the value of  $f(L)$  in the long-length region.<sup>2</sup> Therefore we estimate  $L_{\text{av}}$  to be in the range 125–130 Å.

The value of  $\ell$  reported<sup>12,15</sup> for the drawn sample was obtained from Bragg's law, using a scattering angle from an observed SAXS curve  $I(\theta)$ . In general, it is necessary to correct the observed scattering curve to give the true scattering profile  $I(s)$  through the equation

$$I(s) = \theta^n I(\theta) \quad (6)$$

where  $s = 2\lambda^{-1} \sin \theta$  and where  $\theta^n$  is the "Lorentz factor" in which  $n$  assumes a value ranging from 0 to 2, depending on the nature of the sample.<sup>16</sup> Any value of  $n$  greater than zero will result in a shift of  $\ell$  toward a smaller value. There is controversy in the literature concerning the value of  $n$  appropriate for a drawn fiber.<sup>16</sup> The shift resulting from the correction will be small in any case since, for the extreme value  $n = 2$ , it amounts to less than 30 Å. Therefore  $\ell$  must be in the range 150–180 Å.

The remaining difference between the Raman results (125–130 Å) and the SAXS results (150–180 Å) may reflect in part the presence of an amorphous component and the effect of disorder in the lamellar periodicity on the position and shape of the SAXS curve. The effect of such disorder is a subject that has been considered by a number of authors.<sup>16–20</sup> The most general treatment is by Hosemann,<sup>17</sup> who derived expressions for scattering curves based on a paracrystalline model in which fluctuations in the thickness of both the amorphous and crystalline layers occur. The effects of these fluctuations are to cause the scattering curves to shift position, broaden, and lose intensity, effects that are more pronounced for higher order reflections. The precise way the scattering curves are affected depends critically, however, on the relative amplitude and distribution of the fluctuations.

The "direct" method for analyzing SAXS curves for partially crystalline polymers reported by Strobl<sup>19</sup> is applicable to structures that are relatively well ordered, such as unannealed solution-crystallized polyethylene. For such samples, the ranges of lamellar thicknesses derived from SAXS<sup>19</sup> are consistent with the distribution of straight-

chain segment lengths determined for similar samples from low-frequency Raman measurements.<sup>7</sup> The same approach applied to the drawn sample is made difficult by the absence of an accepted model and by the large fluctuations in lamellar thickness for the fiber relative to those for the solution- and melt-crystallized polymer.

The effect on SAXS curves of paracrystalline-type fluctuations has recently been reviewed by Crist,<sup>16</sup> who very clearly demonstrated that the finite coherence length of the long-period structure severely reduces the maximum of the scattering intensity and makes it eventually unobservable. A variation of the extended length of the chains in the crystal lattice, i.e., the fluctuation and the unevenness of the boundary between the crystalline and amorphous layers, mainly affects the intensity but not very much the position of the scattering maximum. Hence SAXS is a very inadequate tool for the investigation of the distribution of the length of extended chain sections in the crystal blocks, in contrast with the LAM Raman scattering method, which measures just this distribution.

Finally, the presence of conformational defects within the lamellar stems is yet another factor that would tend to affect the Raman and SAXS in a different manner. Such defects would interrupt the all-trans segments to produce shorter, vibrationally uncoupled segments. It appears that a relatively low concentration of such defects could shift  $L_{\max}$  to significantly lower values and account for the presence of the high concentration of straight-chain segments having lengths less than 100 Å. This model will be discussed separately.<sup>21</sup>

**Structure of the Unannealed and Annealed Samples.** The distribution of lengths of straight-chain segments observed for the unannealed drawn sample differs from that for other states of polyethylene in indicating the presence of a large fraction of extended chain segments whose lengths are less than 100 Å. Annealing even at relatively low temperatures (100 °C) results in some reduction in the number of these chains. Further annealing at higher temperatures (127 °C) virtually eliminates the shorter chains and leads to a distribution curve resembling that of an extruded sample.<sup>2</sup> These facts support the view<sup>1</sup> that the morphology of the unannealed drawn fiber is fundamentally different from that of the solution- and melt-crystallized polymer and that this difference is diminished through annealing.

A unique morphology for the unannealed fiber is also indicated by the fact that the half-width  $\Delta L_{1/2}$  of the distribution is anomalously large when compared with values for samples prepared in other ways. In a study to be reported separately,<sup>7</sup> we have found that for solution- and melt-crystallized polyethylene the value of the ratio  $\Delta L_{1/2}/L_{\max}$  varies significantly with  $L_{\max}$ . For  $L_{\max}$  in the vicinity of 100 Å, the ratio is small, for example, 0.1–0.2 for solution-crystallized samples. In contrast, a value near 1.0 is found for the unannealed fiber.

The value of  $\Delta L_{1/2}/L_{\max}$  remained near 1.0 after the sample was annealed at 100 °C. However, after annealing at 127 °C the distribution became more symmetric and shifted to higher  $L$  values. The ratio  $\Delta L_{1/2}/L_{\max}$  was consequently reduced to near 0.85 (Table I), a value that is now in line with the values around 0.7 observed for annealed solution-crystallized samples.

The distribution of straight-chain lengths for the unannealed fiber is characterized by a tail that extends toward long lengths and, in this way, resembles the distribution for the polymer in its extruded state.<sup>2</sup> This tail, which is not present in the case of the solution-crystallized polymer, is probably associated with the extended "taut"

Table II  
Raman Scattering Activities for C-H Stretching Modes of Crystalline Polyethylene<sup>a</sup>

sample	chain orientation	mode	
		d <sup>-</sup> (2885 cm <sup>-1</sup> )	d <sup>+</sup> (2850 cm <sup>-1</sup> )
fiber (cc spectrum)	aligned	0	$\alpha_{zz}^{'2}$
	random	$4/45\beta^{'2}$	$\bar{\alpha}^{'2} + 4/45\beta^{'2}$
poly-crystalline	random	$2/9\beta^{'2}$	$\bar{\alpha}^{'2} + 2/9\beta^{'2}$

<sup>a</sup>  $z$  refers to the chain axis.

tie chains responsible for the high moduli of the fiber and the extrudate. The tail persisted after the fiber was annealed at 127 °C. Because of experimental uncertainties partly associated with corrections for background intensity in the low-frequency (<8 cm<sup>-1</sup>) region, it was not possible, as had been originally hoped, to determine whether or not there was a change in the number of tie chains. This measurement is of importance because it bears on our understanding of the relation between annealing and tensile properties. Thus, it has been observed that a drawn sample annealed with its ends fixed suffers a smaller loss in its initial high elastic modulus than a sample annealed with its ends free.<sup>22</sup> Presumably the greater loss in modulus for the free-end case results from a greater loss in the number of effective tie chains, i.e., those which are fully extended. In our experiment, the sample underwent some slight shrinkage (~5%) during annealing. It appears, however, to have been sufficiently constrained to prevent a sizable loss of tie chains, thus accounting for the persistence of the tail after annealing. On the other hand, it may be that the "effective" tie chains have lengths so great (>600 Å) that their LAM-1 frequencies are beyond the spectral region (<5 cm<sup>-1</sup>) where accurate measurements are possible at present. In any case it is clear that further measurements are needed.

## Summary

(1) The low-frequency LAM-1 band of drawn polyethylene has a shape that distinguishes it from LAM-1 observed for other forms of the polymer: it is exceptionally broad and displays an intense high-frequency wing.

(2) The unique shape of LAM-1 results from a high concentration of short straight-chain segments whose most probable length  $L_{\max}$  is about 90 Å.

(3) The value of  $L_{\max}$  (90 Å) is about one-half the length  $\ell$  of the long period measured by SAXS for similar drawn samples. The difference between these values is reduced when the average length  $L_{av}$  of the straight chains is used for comparison rather than  $L_{\max}$ . The remaining difference between the Raman value (125–130 Å) and the SAXS value (150–180 Å) may be associated with the effects of lattice disorder on the X-ray scattering curve. Another possible contribution to this difference, which would, in addition, account for the presence of the high concentration of short straight-chain segments, involves the presence of conformational defects within the lamellar stems.<sup>21</sup>

(4) The shape of the distribution of lengths of straight-chain segments together with the changes in the shape observed upon annealing the sample shows that the morphology of the unannealed sample is fundamentally different from that of solution- and melt-crystallized samples.

(5) The distribution curve shows a tail extending beyond 500 Å; this tail appears to persist after annealing (127 °C) the sample with its ends fixed.

(6) The extended chains of the unannealed sample were highly aligned in the direction parallel to the draw axis. The average angle of deviation was near  $10^\circ$ . Annealing the sample at  $127^\circ\text{C}$  did not increase the average angle by more than  $2^\circ$ . For comparison, the average angle of deviation for an extruded sample was found to be about  $4.5^\circ$ .

**Acknowledgment.** R.G.S. thanks Stephen J. Krause of the Department of Materials and Metallurgical Engineering at the University of Michigan for valuable discussions concerning the interpretation of SAXS and WAXS data.

## Appendix

To estimate some average deviation of the extended chains from perfect alignment with respect to the fiber axis, we used the peak intensities of two C-H stretching bands: the antisymmetric mode at  $2885\text{ cm}^{-1}$ , which is designated as  $d^-$  and belongs to symmetry species  $B_{1g}$ , and the component of the symmetric mode at  $2850\text{ cm}^{-1}$ , which is designated as  $d^+$  and belongs to species  $A_g$ .<sup>10</sup> Peak intensities have been used since it may be assumed that the shape of a given band is essentially the same for all samples. The calculation has been carried out for two models.

**Two-Component Model.** This model consists of extended chains having random orientations and extended chains having perfect alignment with the fiber axis. We wish to compute the relative fraction of the components. For this purpose we need the relative peak intensities of the  $2885\text{-}$  and  $2850\text{-cm}^{-1}$  bands for the randomly oriented polymer (Figure 6). The relative intensities of bands for the fiber cannot be compared directly with those for the polycrystalline sample because the Raman scattering activities associated with the bands differ for the two samples.<sup>11</sup> The relative intensities of these modes in terms of scattering activities are given in Table II for the fiber and polycrystalline sample.<sup>11,23</sup> Relative values of the terms in the expressions for the  $d^-$  intensities have been determined from measurements on a highly oriented uniaxial sample of extruded polyethylene:  $\alpha_{zz}^{\prime 2}(d^+) = 1.3$ ,  $\bar{\alpha}^{\prime 2}(d^+) = 2.88$ , and  $\beta^{\prime 2}d^+ = 6.70$ . The intensity ratio  $I(2885)/I(2850)$  was found to be equal to 2.00 for the polycrystalline sample. This leads to  $\beta^{\prime 2}(d^-) = 39.3$ . From the cc spectrum of the fiber we can measure the ratio  $r = I(2885)/I(2850)$ . Letting  $x$  represent the fraction of randomly oriented extended chains, we have

$$r = \frac{[\frac{4}{45}\beta^{\prime 2}(d^-)]x}{[\alpha_{zz}^{\prime 2}(d^+)](1-x) + [\bar{\alpha}^{\prime 2}(d^+) + \frac{4}{45}\beta^{\prime 2}(d^+)]x} \quad (\text{A-1})$$

**One-Component Model.** In this model all extended chains are assumed to make the same angle with the draw

axis. Starting with the sample geometry used to measure the cc spectrum (see section on Experiment and Theory), we note that a rotation of the sample about any axis perpendicular to  $c$  introduces into the observed spectrum a dd component. On this basis we may write

$$I(\theta) = I(cc) \cos^2 \theta + I(dd) \sin^2 \theta \quad (\text{A-2})$$

where  $\theta$  is the angle between the chain and fiber axes. Then

$$r = \frac{I^{\text{obsd}}(2885)}{I^{\text{obsd}}(2850)} = \frac{I^{\text{cc}}(2885) \cos^2 \theta + I^{\text{dd}}(2885) \sin^2 \theta}{I^{\text{cc}}(2850) \cos^2 \theta + I^{\text{dd}}(2850) \sin^2 \theta} \quad (\text{A-3})$$

With intensity ratios measured for extruded polyethylene, this equation may be expressed

$$r = 4.40/(\cot^2 \theta + 3.84)$$

## References and Notes

- Peterlin, A. *J. Mater. Sci.* **1971**, *6*, 490.
- Snyder, R. G.; Krause, S. J.; Scherer, J. R. *J. Polym. Sci., Polym. Phys. Ed.* **1978**, *16*, 1593.
- Peticolas, W. L.; Hibler, G. W.; Lippert, J. L.; Peterlin, A.; Olf, H. *Appl. Phys. Lett.* **1971**, *18*, 87.
- Fraser, G. V. *Indian J. Pure Appl. Phys.* **1978**, *16*, 344.
- Kint, S.; Elksen, R. H.; Scherer, J. R. *Appl. Spectrosc.* **1976**, *30*, 281.
- Scherer, J. R. *Appl. Opt.* **1978**, *17*, 1621.
- Snyder, R. G.; Scherer, J. R.; Reneker, D. H.; Colson, J. P., to be submitted for publication.
- Scherer, J. R.; Snyder, R. G. *J. Chem. Phys.* **1980**, *72*, 5798.
- Snyder, R. G.; Scherer, J. R. *J. Polym. Sci., Polym. Phys. Ed.* **1980**, *18*, 421.
- Snyder, R. G.; Scherer, J. R. *J. Chem. Phys.* **1979**, *71*, 3221.
- Snyder, R. G. *J. Mol. Spectrosc.* **1971**, *37*, 353.
- Corneliussen, R.; Peterlin, A. *Makromol. Chem.* **1967**, *105*, 193.
- Olf, H. G.; Peterlin, A.; Peticolas, W. L. *J. Polym. Sci., Polym. Phys. Ed.* **1974**, *12*, 359.
- Koenig, J. L.; Tabb, D. L. *J. Macromol. Sci., Phys.* **1974**, *9*, 141.
- Peterlin, A.; Corneliussen, R. *J. Polym. Sci., Part A-2* **1968**, *6*, 1273.
- Crist, B. *J. Polym. Sci., Polym. Phys. Ed.* **1973**, *11*, 635.
- Hosemann, R.; Bagchi, S. N. "Direct Analysis of Diffraction of Matter"; North-Holland Publishing Co.: Amsterdam, 1962.
- Crist, B.; Morosoff, N. *J. Polym. Sci., Polym. Phys. Ed.* **1973**, *11*, 1023.
- Strobl, G. R. *J. Appl. Crystallogr.* **1973**, *6*, 365. Strobl, G. R.; Müller, N. *J. Polym. Sci., Polym. Phys. Ed.* **1973**, *11*, 1219.
- Reinhold, C.; Fischer, E. W.; Peterlin, A. *J. Appl. Phys.* **1964**, *35*, 71.
- Peterlin, A.; Snyder, R. G., submitted for publication in *J. Polym. Sci., Polym. Phys. Ed.*
- Peterlin, A. "Ultra High Modulus Polymers"; Ciferri, A., Ward, I. M., Eds.; Applied Science Publishers: London, 1979; Chapter 10.
- Wilson, E. B., Jr.; Decius, J. C.; Cross, P. C. "Molecular Vibrations"; McGraw-Hill, New York, 1955; Chapter 3.
- Reference to a company and/or product is only for purposes of information and does not imply approval or recommendation of the product by the Department of Agriculture or the National Bureau of Standards to the exclusion of others which may also be suitable.